Polymer 51 (2010) 3899–3906

Contents lists available at ScienceDirect

Polymer

journal homepage: www.elsevier.com/locate/polymer

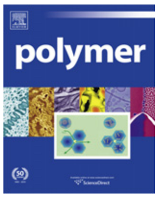

Organo-soluble phosphinated polyimides from asymmetric diamines

Ching Hsuan Lin*, Sheng Lung Chang, Li An Peng, Siao Ping Peng, Yu Hao Chuang

Department of Chemical Engineering, National Chung Hsing University, Taichung 402, Taiwan

ARTICLE INFO

Article history:
Received 3 November 2009
Received in revised form
17 May 2010
Accepted 29 May 2010
Available online 19 June 2010

Keywords:
Asymmetric
One-pot
Phosphinate

ABSTRACT

Two new asymmetric diamines (**1**–**2**) were prepared via a facile, one-pot procedure. Based on diamine (**1**–**2**), a series of asymmetric polyimides (**3**–**4**) were prepared in NMP/xylene by high-temperature solution polymerization. The resulting polyimides are readily soluble in some organic solvents, and can be solution casted into flexible and creasable films. An intramolecular charge complex mechanism was proposed to the structure–optical transparency relationship. Polyimides **3**–**4** display high-Tg (319–401 °C), high moduli (2.40–7.20 GPa), moderate coefficient of thermal expansion (38–53 ppm/°C), and excellent flame retardancy. These results show that the introduction of the asymmetric structure is an effective way to improve organo-solubility while maintaining thermal properties. Because of these properties, polyimides **3**–**4** can be considered as excellent high-Tg and flame-retardant materials for microelectronic applications.

1. Introduction

Aromatic polyimides are well-known as heat-resistant material and have been widely applied in electronics, optics, and composites [1]. However, aromatic polyimides are difficult to process because of their insolubility and infusibility. As a result, the processing of polyimides is generally carried out by a two-step procedure. The first step is the reaction of dianhydride and diamine in polar aprotic solvent, forming poly(amic acid). The second step is the thermal imidization of poly(amic acid) to polyimide. However, from a industrial viewpoint, the strict moisture limitation in the first step, and the storage instability of poly(amic acid) are drawbacks of the two-step procedure. This prompts the development of one-step high-temperature solution polymerization procedure, in which m-cresol or NMP/xylene is employed as solvent [2–5]. In the m-cresol system, the condensed water is blown away or repelled from m-cresol at elevated temperature since it has much lower boiling point than m-cresol. In the NMP/xylene system, condensed water is distillated via azeotrope distillation of water/xylene during polymerization. One feature of high-temperature solution polymerization is that it is suitable for diamines with low reactivity at low temperatures. The other feature of the one-step procedure is that the limitation of water content in solvent is not as strict as that in the two-step procedure because the excess water will be distillated during azeotrope distillation. However, if the resulting polyimide is not soluble in the solvent, precipitate will form during polymerization, leading to a polyimide with low molecular weight. As a result, the prerequisite of solution polymerization is that the resulting polyimide must be soluble in the solvent.

Studies have reported that incorporating bulky pendant [6–12] into polymer chains can impart better organo-solubility because of the decreased packing density and crystallinity. Other studies have reported that phosphorus-functionalized polymers, whether in the phosphine oxide form [13–17], in the phosphonate [18,19] or in the phosphinate form [20–28], can improve organo-solubility, adhesion to metal, flame retardancy and atomic oxygen resistance. As a result, polyimides with bulky phosphorus pendant seem to be a good strategy for better organo-solubility and flame retardancy. Recently, we reported a phosphinate-functionalized polyimides [10] and poly(ether imides) [25]. However, although a bulky pendant [10,25] or two ether linkages were present [25], the organo-solubility of the resulting polyimides was not good. Studies have shown that incorporating asymmetric structure into polymer chains can impart better organo-solubility because of the disturbed sequence distribution [29–36]. Herein, with our continuing effort to prepare organo-soluble polyimides with excellent flame retardancy, two asymmetric diamines, 1-(4-aminophenyl)-1-(3,5-dimethyl-4-aminophenyl)-1-(6-oxido-6H-dibenz <c,e> <1,2> oxaphosphorin-6-yl) ethane (**1**) and 1-(4-aminophenyl)-1-(3,5-diethyl-4-aminophenyl)-1-(6-oxido-6H-dibenz <c,e> <1,2> oxaphosphorin-6-yl)ethane (**2**), were developed. Based on diamines (**1**–**2**), a series of polyimides (**3**–**4**) were prepared from the condensation of (**1**–**2**) with various aromatic dianhydrides in NMP/xylene by high-temperature solution polymerization. We then investigated the chemical structures,

---

* Corresponding author. Tel.: +886 4 22850180; fax: +886 4 22854734.
E-mail address: linch@nchu.edu.tw (C.H. Lin).

0032-3861/$ – see front matter © 2010 Elsevier Ltd. All rights reserved.
doi:10.1016/j.polymer.2010.05.059

solubility, crystallinity, and thermal properties of polyimides **3**–**4**. This study also discusses the electron-withdrawing/donating effect of 2,6-disubstituted aniline on the preparation of asymmetric diamines (**1**–**2**) and (**5**). In addition, properties such as organosolubility, optical transparency, and thermal properties of asymmetric polyimides were discussed and the structure–property relationship was discussed.

2. Experimental

2.1. Materials

9,10-Dihydro-oxa-10-phosphaphenanthrene-10-oxide (DOPO, TCI), 4-aminoacetophenone (Acros), 2,6-dimethylaniline (Acros), 2,6-diethylaniline (Acros), 2,6-difluoroaniline (Acros), p-toluenesulfonic acid monohydrate (p-TSA, Showa) were used as received. Pyromellitic dianhydride (PMDA, Acros) was dried at 170 °C overnight before use. 3,3′,4,4′-Benzophenonetetracarboxylic dianhydride (BTDA, Acros), 4,4′-oxydiphthalic anhydride (ODPA, Chriskev), and 3,3′,4,4′-biphenyltetracarboxylic dianhydride (BPDA, Chriskev) were recrystallized from acetic anhydride. The solvents used are commercial products (HPLC grade) and were used without further purification.

2.2. Characterization

NMR measurements were performed using a Varian Inova 600 NMR in DMSO-d_6, and the chemical shift was calibrated by setting the chemical shift of DMSO-d_6 as 2.49 ppm. IR spectra were obtained in the standard wavenumber range of 400–4000 cm^{-1} by Perkin–Elmer RX1 infrared spectrophotometer. High-resolution mass (hr-ms) measurements were performed by a Finnigan/Thermo Quest MAT 95XL mass spectrometer by fast atom bombardment. Elemental analysis was performed on an Elementar Vario EL III. Wide-angle X-ray diffraction measurements were performed at room temperature by a MAC Science DMAX2000 X-ray diffractometer with monochromatic Cu Ka radiation ($\lambda = 1.5418$ Å, operating at 40 kV and 30 mA). The scanning rate was 3°/min over a range of $2\theta = 5–40°$. Differential scanning calorimeter (DSC) scans were obtained by a Perkin–Elmer DSC 7 in a nitrogen atmosphere at a heating rate of 20 °C/min. Tg was taken as the midpoint of the heat capacity transition between the upper and lower points of deviation from the extrapolated liquids and glass lines. Dynamic mechanical analysis (DMA) was performed with a Perkin–Elmer Pyris Diamond DMA with a sample size of $5.0 \times 1.0 \times 0.002$ cm. The storage modulus E' and tan δ were determined as the sample was subjected to the temperature scan mode at a programmed heating rate of 5 °C/min at a frequency of 1 Hz. The test was performed by tension mode with an amplitude of 25 μm. Thermo mechanical analysis (TMA) was performed by a SII TMA/SS6100 at a heating rate of 5 °C/min. The coefficient of thermal expansion (CTE) was measured in the range from 100 °C to 250 °C. Thermal gravimetric analysis (TGA) was performed by a Seiko Exstar 600 at a heating rate of 20 °C/min in a nitrogen atmosphere from 105 °C to 800 °C. Gel permeation chromatography (GPC) was carried out on a Hitachi L2130 with a UV detector (L2400) using *N*,*N*-dimethylformamide (DMF) as the eluent at 60 °C with a flow rate of 1.0 mL/min. The data were calibrated with polystyrene standard.

Optical rotation is detected by a Perkin–Elmer 241 polarimeter. Flame retardancy of polyimides was performed by a UL-94VTM vertical thin test. In that test, an 8" × 2" sample was wrapped around a 1/2" mandrel, and then taped on one end. The mandrel was removed, leaving a cone-shaped sample that was relatively rigid. The two flame applications were 3 s instead of 10 s. After the first ignition, the flame was removed and the time for the polymer to self-extinguish (t_1) was recorded. Cotton ignition was noted if polymer dripping occurred during the test. After cooling, the second ignition was performed on the same sample and the self-extinguishing time (t_2) and dripping characteristics were recorded. If t_1 plus t_2 was less than 10 s without any dripping, the polymer was considered to be a VTM-0 material. If t_1 plus t_2 was in the range of 10–30 s without any dripping, the polymer was considered to be a VTM-1 material.

2.3. Synthesis of (**1**)

DOPO 25.94 g (0.12 mol), 2,6-dimethylaniline 46.14 g (0.36 mol), 4-aminoacetophenone 16.46 g (0.12 mol), and p-TSA 1.038 g (4 wt% of DOPO) were introduced into a 250 mL round-bottom glass flask equipped with a nitrogen inlet and a magnetic stirrer. The reaction mixture was stirred at 130 °C for 24 h. After that, the precipitate was filtered and recrystallized from methanol, and then dried in a vacuum oven at 150 °C for 8 h. Light white crystal (75% yield) with a melting point of 280 °C (DSC) was obtained. HR-MS(FAB+) *m*/*z*: calcd. for $C_{28}H_{27}O_2N_2P$ 454.1810; anal., 455.1898 $(M + 1)^+$, $C_{28}H_{28}O_2N_2P$. Elemental analysis of $C_{28}H_{27}O_2N_2P$: calculated C, 73.99%; H, 5.99%; N, 6.16%. Found: C, 73.77%; H, 5.69%; N, 5.93%. ^{1}H NMR (DMSO-d_6), δ = 1.51 (3H,H^6), 1.94 (6H,H^{22}), 4.43 (2H,NH_2), 5.04 (2H,NH_2), 6.43 (2H,H^2), 6.81 (2H,H^{20}), 7.01 (2H,H^3), 7.11 (1H, H^{11}), 7.14 (1H,H^{17}), 7.16 (1H,H^{15}), 7.32 (1H,H^{10}), 7.34 (1H,H^{16}), 7.64 (1H,H^9), 7.95 (1H,H^{14}), 8.04 (1H,H^8). ^{13}C NMR (DMSO-d_6), δ = 18.11 (C^{22}), 24.21 (C^6), 51.45 (C^5), 113.09 (C^2), 118.85 (C^{17}), 119.80 (C^{12}), 120.93 (C^{13}), 122.99 (C^7), 123.12 (C^8), 123.65 (C^{15}), 125.23 (C^{14}), 126.40 (C^{16}), 127.62 (C^{10}), 128.05 (C^{20}), 129.43 (C^3), 130.05 (C^{21}), 130.45 (C^{19}), 131.89 (C^{11}), 132.97 (C^9), 135.96 (C^4), 142.56 (C^{23}), 147.29 (C^1), 150.81 (C^{18}). ^{31}P NMR, (DMSO-d_6), δ = 42.4(s). The synthesis of diamine (**1**) is shown in Scheme 1.

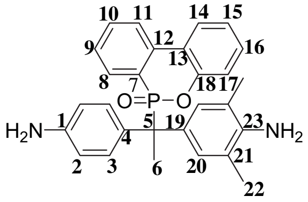

2.4. Synthesis of (**2**)

Diamine (**2**) was synthesized with a procedure similar to (**1**) using 2,6-diethylaniline as the starting material. White crystal (70% yield) with a melting point of 246 °C (DSC) was obtained. HR-MS (FAB+) *m*/*z*: calcd. for $C_{30}H_{31}O_2N_2P$ 482.2123; anal., 483.2199 $(M + 1)^+$, $C_{30}H_{32}O_2N_2P$. Elemental analysis of $C_{30}H_{31}O_2N_2P$: calculated C, 74.67%; H, 6.48%; N, 5.81%. C, 74.21%; H, 6.66%; N, 5.79%. ^{1}H NMR (DMSO-d_6), $\delta = 0.99$ (3H,H^{23}), 1.57 (3H,H^6), 2.30 (2H,H^{22}), 1.94 (6H,H^{22}), 4.41 (2H,NH_2), 5.03 (2H,NH_2), 6.43 (2H,H^2), 6.80 (2H,H^{20}), 7.04 (2H,H^3), 7.07 (1H,H^{11}), 7.12 (1H,H^{15}), 7.22 (1H,H^{17}), 7.32 (1H, H^{10}), 7.34 (1H,H^{16}), 7.63 (1H,H^9), 7.91 (1H,H^{14}), 8.02 (1H,H^8). ^{13}C NMR (DMSO-d_6), $\delta = 13.18$ (C^{23}), 23.88 (C^{22}), 24.42 (C^6), 51.35 (C^5), 113.04 (C^2), 118.73 (C^{11}), 120.90 (C^{12}), 122.72 (C^7), 123.18 (C^8), 123.57 (C^{15}), 125.23 (C^{14}), 125.64 (C^{20}), 126.05 (C^{13}), 126.54 (C^{21}), 127.63 (C^{10}), 129.45 (C^{19}), 130.05 (C^3), 130.41 (C^{16}), 131.84 (C^{17}), 132.93 (C^9), 135.95 (C^4), 141.19 (C^{24}), 147.24 (C^1), 150.75 (C^{18}). ^{31}P NMR (DMSO-d_6), $\delta = 38.5$(s). The synthesis of diamine (**2**) is shown in Scheme 1. Data from single crystal diffractogram of (**2**) were listed in Supporting information.

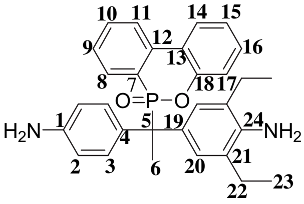

2.5. Preparation of polyimides

Polyimides syntheses are exemplified by the synthesis of **3a** from the condensation of (**1**) and PMDA. To a 100-mL three-neck round-bottom flask equipped with a magnetic stirrer, a Dean–Stark trap, and a nitrogen inlet, (**1**) 1.3536 g (3 mmol), PMDA 0.6544 g (3 mmol) and NMP 7.0 g were added. After the monomer had dissolved completely, xylene 7 g was added. The reaction was carried out at reflux temperature for 12 h. Then, the viscous polyimides solution was casted on glass by an automatic film applicator, and dried at 80 °C overnight and 100 °C (1 h), 200 °C (2 h), respectively. The other polyimides (**3b**–**3d**, **4a**–**4d**) were similarly prepared. The synthetic equation of polyimides **3**–**4** is shown in Scheme 2.

3. Results and discussion

3.1. Synthesis of (**1**–**2**)

Asymmetric diamine (**1**–**2**) were prepared by a one-pot reaction of DOPO, 4-aminoacetophenone in excess 2,6-dimethylaniline (or 2,6-diethylaniline) using p-TSA as the catalyst. The excess 2,6-dimethylaniline (or 2,6-diethylaniline) played the roles of both reactant and reaction medium. Generally, aromatic diamines are prepared from reduction of their nitro-containing precursors, except for those prepared acid catalyzed condensation of ketone or aldehyde compounds with excess aniline [37–39]. However, catalytic hydrogenation requires high pressure, an expensive palladium-on-carbon catalyst, and large investment in facilities for industrial-scale production. Thus, this non-reduction, one-pot synthesis makes diamines (**1**–**2**) attractive for to industrial applications. Although some aromatic diamines can also be prepared by a one-pot procedure [37–39], however, only symmetric diamines can be obtained. In this work, asymmetric diamines can easily be prepared by using 2,6-disubstituted aniline as reactant. To the best of our knowledge, this is the first case of producing asymmetric diamines in a one-pot procedure. In addition to (**1**–**2**), we also attempted to prepare asymmetric diamine (**5**) using 2,6-difluoroaniline as a starting material (Scheme 3). However, the synthesis was unsuccessful under various acidic conditions. According to ^{1}H NMR analysis of the reaction product, the methyl signal (H^{6}) was disappeared. Obviously, the electron-withdrawing fluoro groups deactivated the electrophilicity of aniline for the electrophilic substitution. The disappearance of methyl signal (H^{6}) suggests that an elimination reaction between the methyl and hydroxy groups occurred in acidic conditions. Detailed researches for the elimination reaction in acidic conditions and synthesis of (**5**) in basic condition [40] are under investigation. From above discussion, the electron-donating or electron-withdrawing characteristic of 2,6-disubstituents is crucial for the proceeding of electrophilic substitution. 2,6-Disubstituted aniline with the electron-donating methyl or ethyl groups can carry out the electrophilic substitution. In contrast, 2,6-disubstituted aniline with the electron-withdrawing fluoro group cannot accomplish the electrophilic substitution.

3.2. Characterization of (**1**–**2**)

Fig. 1 shows the ^{1}H NMR spectra of (**1**). Two amino peaks at 5.0 and 4.4 ppm confirm the asymmetric structure of diamine (**1**). The signals of methyl group at 1.5 ppm were split into two peaks with a coupling constant of 17.4 Hz because of a $^{3}J_{P-H}$ coupling. The assignment of Ar–H, assisted by the correlations in the ^{1}H–^{1}H COSY NMR spectrum (Fig. 2) (Fig. S1) confirms the structure of (**1**). In the ^{13}C NMR spectrum, due to the P–C ^{1}J coupling, the signals of C^{5} were split into two peaks at 51.1 and 51.8 ppm with a coupling constant of 105 Hz. The signals of C^{7} were also split into two peaks at 122.6 and 123.4 ppm with a coupling constant of 120 Hz for the same reason. The assignment of Ar–C, assisted by the correlations in the ^{1}H–^{13}C HETCOR NMR spectrum (Fig. S2) also confirms the structure of (**1**). In the ^{31}P NMR spectrum, only one ^{31}P NMR peak was observed at 42.4 ppm, indicating both the purity and the integrity (no ring opening) of the biphenylene phosphinate pendant. ^{1}H, ^{13}C, ^{1}H–^{1}H COSY and ^{1}H–^{13}C HETCOR NMR spectra of (**2**) were reported in the supplementary information (Figs. S3–S6), and the spectroscopic data supported the structure of (**2**).

Since the phosphorus and aliphatic carbon in diamines (**1**–**2**) are both chiral centers, four stereoisomers should result. Theoretically, each stereocenter can be either R or S configuration, and hence, the possible combinations are RR, RS, SR, and SS configurations. The four stereoisomers can be grouped into two pairs of enantiomers, resulting in two pairs of diastereomers: RR + SS and RS + SR. The RR stereoisomer is the enantiomer of the SS stereoisomer, and is diastereomerically related to the RS and SR stereoisomers. In contrast with enantiomers, diastereomers are distinct molecules with different physical and chemical properties because they are not mirror images of each other. However, according to the ^{1}H and ^{13}C NMR spectra of (**1**–**2**), there is no evidence shown that two pairs of diastereomers were obtained in this synthesis. In addition, no optical rotation is observed in a polarimeter. That is, only racemic mixture with equal RR and SS configurations, or equal RS and SR configurations were obtained. At this stage, no reasonable explanation is provided. A more detailed research is required to explain this phenomenon.

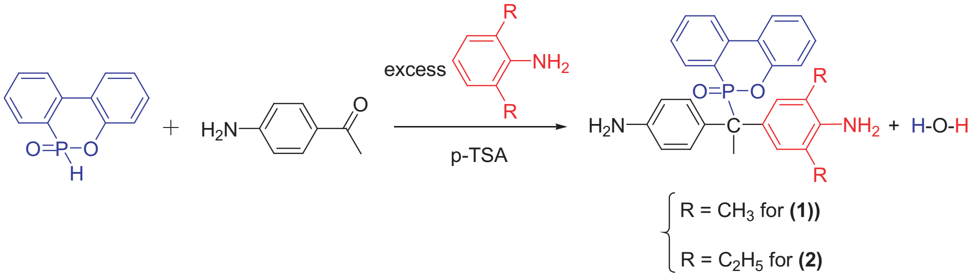

Scheme 1. One-pot synthesis of diamine (**1**–**2**).

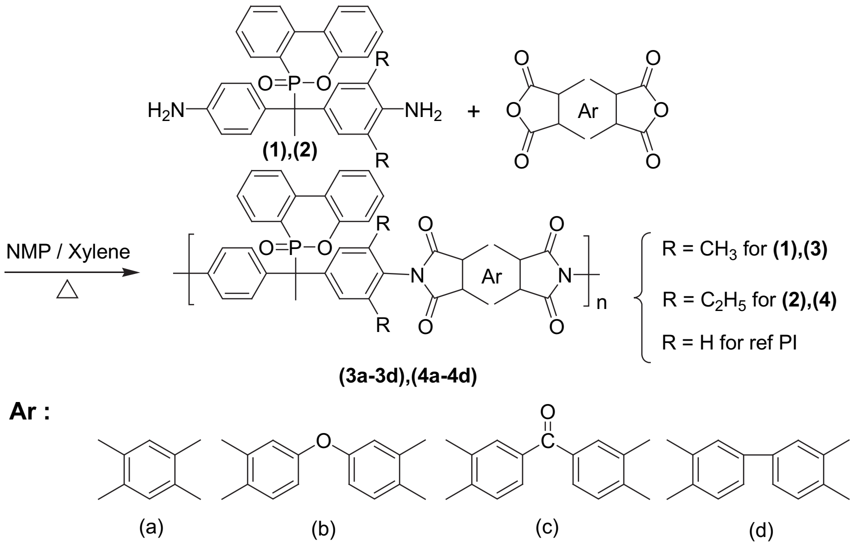

Scheme 2. Synthesis of polyimides **3**–**4**.

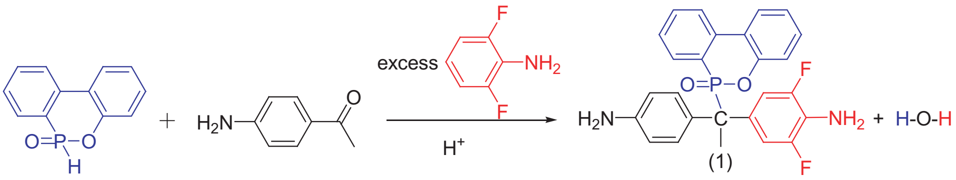

Scheme 3. Synthesis of diamine (**5**). However, the synthesis is unsuccessful due to poor reactivity of 2,6-difluoroaniline.

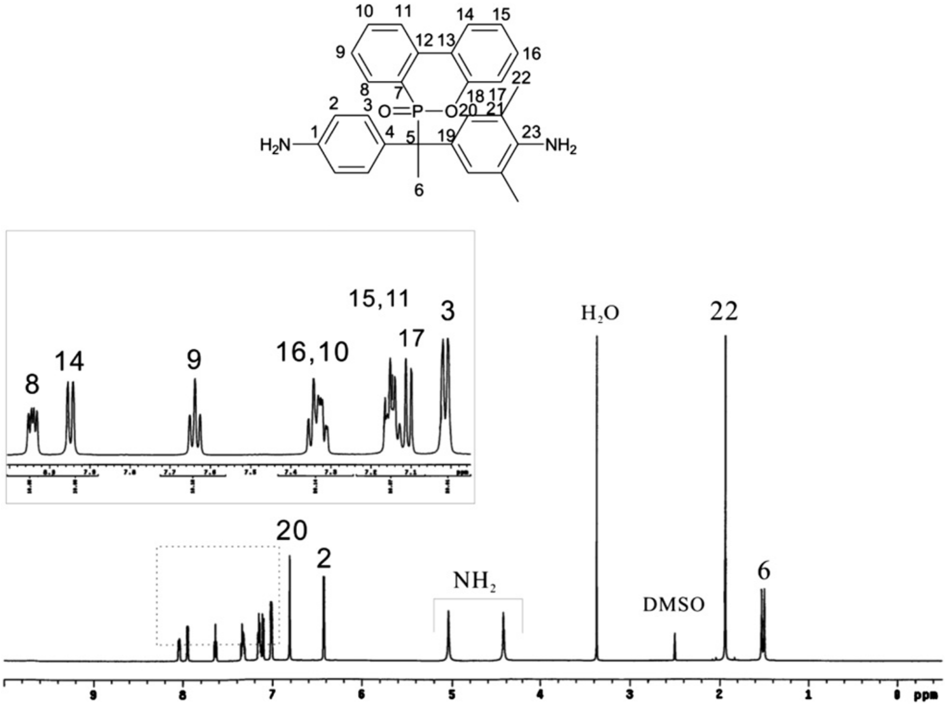

Fig. 1. ^{1}H NMR spectrum of diamine (**1**).

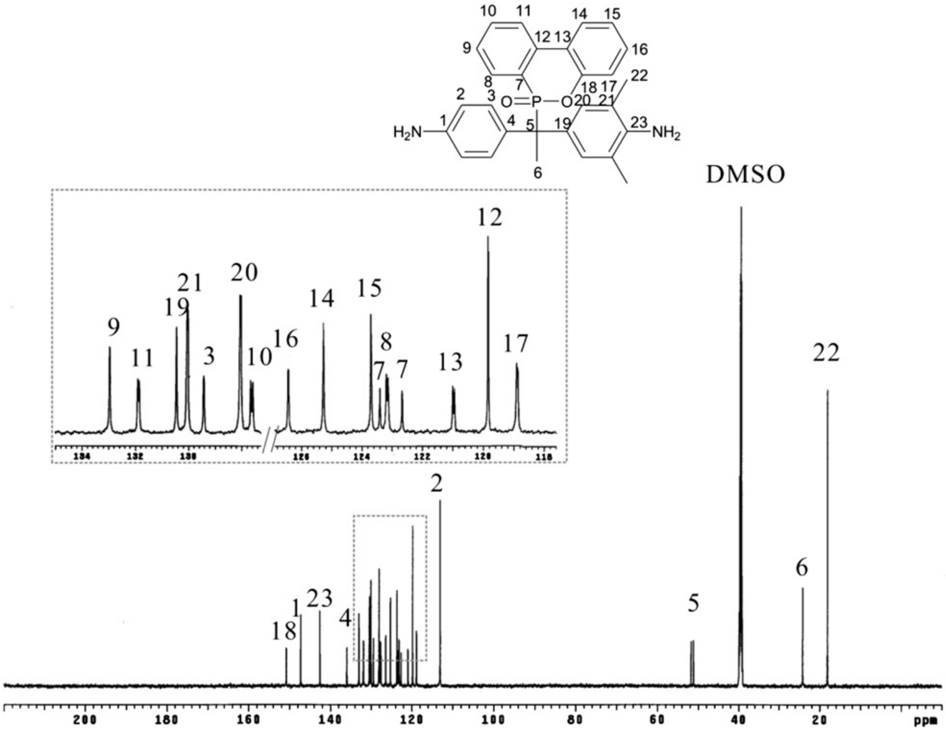

Fig. 2. ^{13}C NMR spectrum of diamine (**1**).

3.3. *Polyimide synthesis*

Polyimides **3**–**4** were prepared by reacting (**1**–**2**) with equal mole of dianhydrides (**a**–**d**) in NMP/xylene by high-temperature solution polymerization. According to the principle of NMR, a larger chemical shift of an amino proton means a lower electron density of amino group, and corresponds to a lower reactivity. The chemical shifts of the amino group of (**1**–**2**) are around 5.0 and 4.4 ppm, which is similar to that (5.0 ppm) diaminodiphenylmethane. This suggests that, from the viewpoint of electron density, the reactivity of (**1**–**2**) is high. Initially, we prepared polyimides **3**–**4** via the standard two-step procedure. However, the viscosity of poly(amic acid) in the first step was not very high. We speculated that the steric hindrance resulting from the dimethyl groups reduced the reactivity. Therefore, a high-temperature solution polymerization was applied to overcome the steric hindrance. However, to prevent precipitate during polymerization, the polyimides should be soluble in the solvent. In this case, the bulky pendant, together with the asymmetric linkage, makes polyimides **3**–**4** soluble in the reaction solvent. In the IR spectrum of **3a**, the characteristic peaks of imide at 1776 cm^{-1} (C=O asymmetric stretch) and 1723 cm^{-1} (C=O symmetric stretch), 1379 cm^{-1} (C–N stretch), 1113 and 721 cm^{-1} (imide ring deformation) confirm the complete imidization. The peaks of P=O absorption at 1202 cm^{-1}, and P–O–Ph absorption at 923 cm^{-1} indicate that the biphenylene phosphinate pendant did not cleave. As listed in Table 1, the number-average molecular weights range from 1.7 to 5.9 × 10^4 g/mol, and the weight-average molecular weights range from 3.2 to 8.9 × 10^4 g/mol, demonstrating moderate-to-high molecular weight, and reflecting high-purity and reactivity of (**1**–**2**) at high temperature.

Table 1
Molecular weight and solubility data of polyimides **3**–**4**.

Polyimides	GPC data[a]		Solubility data[c]							
	M_n[b] × 10^{-4}	M_w × 10^{-4}	NMP	DMAc	DMF	DMSO	m-Cresol	$CHCl_3$	CH_2Cl_2	THF
3a	1.7	3.5	+(±)[d]	+(±)	+(±)	+h(−)	+(+)	+h(−)	+(−)	−(−)
3b	2.9	5.2	+(±)	+(±)	+(±)	+(−)	+(±)	+(+)	+(+)	−(−)
3c	3.8	8.5	+(±)	+(±)	+(±)	+h(−)	+(±)	+h(−)	±(−)	−(−)
3d	3.4	6.7	+(±)	+(±)	+h(±)	+h(−)	+(+)	+(±)	+(±)	−(−)
4a	1.7	3.2	+	+	+	+	+	+	±	±
4b	3.1	5.1	+	+	+	+	+	+	+	+
4c	4.9	8.5	+	+	+	+	+	+	+	±
4d	5.9	8.9	+	+	+	+h	+	+	+	±

[a] Relative to polystyrene standard, using DMF as eluent.

[b] M_n: number-average molecular weight, M_w: weight-average molecular weight.

[c] Solubility was tested with a 5 mg sample in 0.5 g of solvent at room temperature. +, soluble; +h, soluble on heating; ±, partially soluble on heating; −, insoluble on heating.

[d] Data in parentheses are those of reference polyimides.

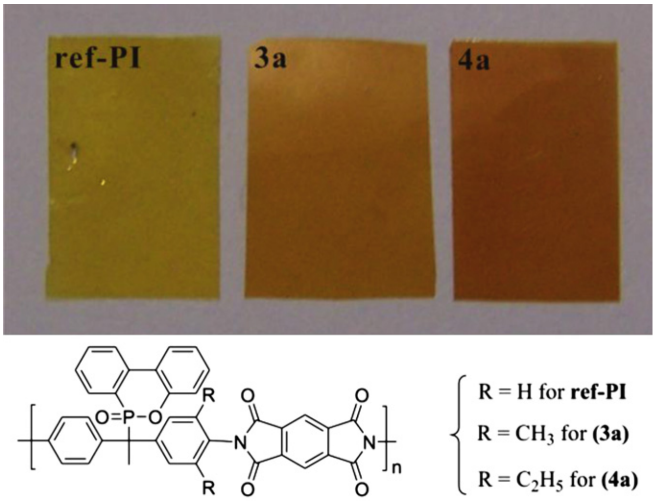

Fig. 3. Pictures of ref PI, **3a** and **4a**.

3.4. *Properties of the polyimides*

3.4.1. *Organo-solubility and crystallinity*

The solubility data of polyimides **3**–**4** are listed in Table 1. As shown in Table 1, asymmetric polyimides **3**–**4** display better organo-solubility than the ref PIs. The asymmetric structure, which leads to the formation of configuration isomers of the repeat unit and resulted in the disruption of packing sequence, should be responsible for the improved solubility. Among them, polyimides **4** show better solubility than polyimides **3** due to the increased free volume caused by ortho-diethyl groups. According to the patterns of wide-angle X-ray diffraction of polyimides **3**–**4** (Fig. S7), all polyimides are amorphous. The bulky biphenylene phosphinate, together with the asymmetric linkage, should be responsible for the amorphous characteristic and improved solubility.

3.4.2. *Film quality and color*

Fig. 3 shows pictures of ref PI, **3a** and **4a**. All polyimide films are creasable and tough although no flexible ether linkages were present in their structure. Generally, polyimide films are typically yellow to amber in color, and the intermolecular charge-transfer complex (CTC) formation is responsible for the color. It has been reported that the intermolecular CTC formation can be reduced by introducing a bulky pendant group to prevent the polyimide chains from being well-stacked [41,42]. However, as presented in the picture, although a bulky phosphinate and two alkyl pendants were presented, polyimides **3a** and **4a** are not transparent enough, and are even darker than the ref PI, in which no alkyl groups were presented. Obviously, the dialkyl groups have negative effect on the transparency of phosphinate polyimides. The reason might be explained by the unusual orientation of phosphinate pendant shown in the single crystal diffractogram of (**2**) (Fig. 4). Instead of being distant from the diethyl groups to reduce the steric and electronic repulsion, the phosphinate inclined to the diethyl groups. As a result, it is speculated that the unusual orientation is related to the interaction between phosphorus and diethyl groups. Judging from the structure of (**2**), the phosphorus element is electron-deficient due to the electron-withdrawing effect of two adjacent oxygen atoms. In contrast, the diethyl groups are electron-donating groups, which can stabilize the electron-deficient phosphorus via a intramolecular interaction. As a result, the intramolecular interaction explained the unusual orientation of phosphinate pendant. At present, it is speculated that the charge-transfer complex should be responsible for the darker colors of polyimides **3**–**4**. However, a detailed investigation is needed to prove the speculation.

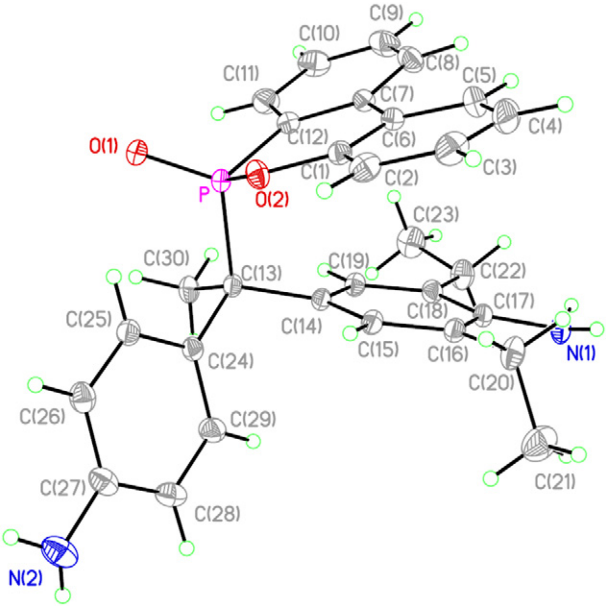

Fig. 4. Single crystal diffractogram of (**2**).

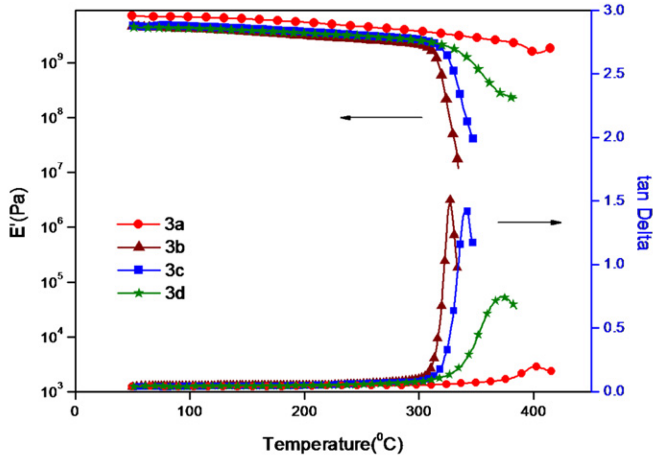

Fig. 5. DMA thermograms of polyimides **3**.

3.4.3. *Dynamic and thermal mechanical properties*

Since polyimides **3**–**4** are flexible and creasable, DMA and TMA were applied to evaluate their thermal mechanical properties and dimensional stability. Fig. 5 shows the DMA thermograms of polyimides **3**. The Tg obtained from the peak temperature of tan(δ) is as high as 401, 327, 341 and 371 °C for **3a**–**3d**, respectively. Compared with Tgs of the ref PIs (Table 2), one can find Tgs of polyimide **3** are enhanced. This result indicates that the ortho-dimethyl groups hinder the rotation of polyimide chains, and thus explains the higher Tg phenomenon. However, as listed in Table 2, Tgs were reduced when ortho-diethyl groups instead of ortho-methyl groups were incorporated. The increased free volume and flexibility of ethyl group may be responsible for the reduced Tg. Fig. 6 shows a typical TMA curve of **3b**. A CTE of 38 ppm/°C was obtained, which is relatively low for an organo-soluble polyimide without bi-axial orientation. Table 2 lists TMA data of other polyimides. The CTEs of polyimides **3** ranged from 38 to 48 ppm/°C, and Tgs from TMA

Table 2
Thermal and mechanical properties of polyimides **3**–**4**.

Polymer	Film quality	E' (GPa)[a]	Tan δ (°C)[a]	Tg (°C) (TMA)[b]	CTE[c] (ppm/°C)	Td$_5$[d] (°C)		Char yield (%)[e]	
						N$_2$	Air	N$_2$	Air
3a	Creasable	7.20	401 (392)[f]	390 (388)[f]	43 (42)[f]	460	443	57	52
3b	Creasable	4.64	327 (318)	317 (304)	48 (48)	449	444	56	47
3c	Creasable	4.72	341 (326)	328 (312)	44 (50)	448	445	57	51
3d	Creasable	4.46	371 (343)	351 (330)	38 (43)	453	438	59	46
4a	Creasable	4.63	365	–	51	454	433	59	51
4b	Creasable	2.76	319	307	53	441	434	56	45
4c	Creasable	4.25	329	317	42	461	445	58	51
4d	Creasable	2.40	347	332	42	459	433	58	45

[a] Measured by DMA; heating rate, 5 °C/min; storage modulus (E′) are recorded at 50 °C.
[b] Measured by TMA; heating rate, 10 °C/min.
[c] Coefficient of thermal expansion is recorded at 100–250 °C.
[d] The 5% decomposition temperature.
[e] Residual wt% at 800 °C in nitrogen.
[f] Data in parentheses are those of reference polyimides.

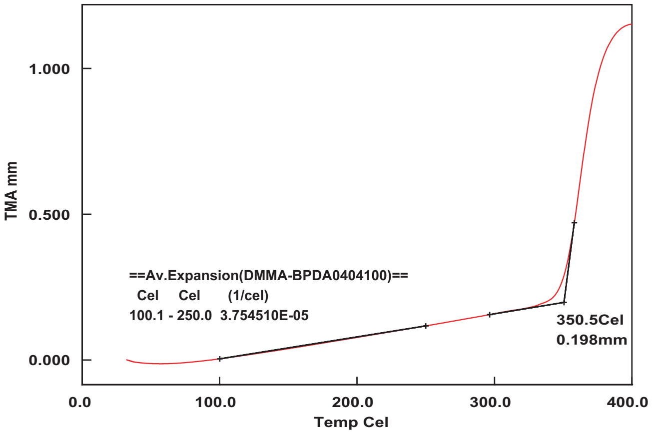

Fig. 6. TMA curve of **3b**.

ranged from 317 to 390 °C (Table 2). Compared with those of reference polyimides, Tg and CTE of polyimides **3** are both enhanced, displaying the high-Tg characteristic and good dimensional stability of ortho-dimethyl substituted polyimides. In contrast, the CTE of polyimides **4** was slightly higher than those of polyimide **3**. The result may also be attributed to the increased free volume caused by ortho-diethyl group (Fig. 6).

3.4.4. Thermal stability and flame retardancy

The thermal stability of polyimides **3**–**4** was evaluated by TGA (Table 2). The 5 wt% degradation temperatures range from 441 to 460 °C in the nitrogen atmosphere and range from 433 to 445 °C in the air atmosphere, demonstrating moderate-to-high thermal properties. As to the flame retardancy, according to the UL-94VTM vertical thin test, the $t_1 + t_2$ is less than 4 s for polyimides **3**–**4**, so they belong to the VTM-0 grade. Although wholly aromatic polyimides usually possess VTM-0 grade without halogen and phosphorus components, they are usually organo-insoluble. The combination of organo-solubility and flame retardancy makes polyimides **3**–**4** attractive for industrial application.

4. Conclusions

We have prepared a series of asymmetric polyimides based on asymmetric diamines (**1**–**2**), which were prepared by a one-pot procedure. To the best of our knowledge, this is the first case of producing asymmetric diamines in a one-pot procedure. In contrast to the electro-donating dialkyl groups that activate the electrophilic substitution, the electron-withdrawing difluoro groups deactivate the electrophilic substitution. This explains the difficulty in preparing diamine (**5**). The asymmetric polyimides **3**–**4** display better organo-soluble property than the ref PIs. The asymmetric structure, which leads to the formation of configuration isomers of the repeat unit and results in the disruption of packing sequence, is responsible for the improved solubility. Although a bulky phosphinate and two alkyl pendant were presented, polyimides **3**–**4** are not transparent enough, and are even darker than the ref PIs. From the unusual orientation of phosphinate pendant shown in the single crystal diffractogram of (**2**), it is thought that the darker color of polyimides **3**–**4** is due to the intramolecular charge-transfer complex. Even though with darker color, the combination of flexibility, high glass transition temperature, improved organo-solubility, and excellent flame retardancy makes polyimides **3**–**4** promising polymers electronic applications, such as in halogen-free flexible copper clad laminate.

Appendix. Supplementary data

Supplementary data associated with this article can be found in online version at doi:10.1016/j.polymer.2010.05.059.

References

[1] Mittal KL, editor. Polyimides: synthesis, characterization, application, vols. 1 and 2. New York: Plenum Press; 1984.
[2] Harries FW, Hsu SL-C. High Perform Polym 1989;1:1.
[3] Cheng SZD, Arnold Jr FE, Zhang A, Hsu SL-C, Harries FW. Macromolecules 1991;24:5856–62.
[4] Fu GD, Kang ET, Neoh KG, Lin CC, Liaw DJ. Macromolecules 2005;38:7593–600.
[5] Luo J, Haller M, Li H, Tang HZ, Jen AK-Y, Jakka K, et al. Macromolecules 2004;37:248–50.
[6] Kricheldorf HR, Fna SC, Vakhtangishvili L, Schwarz G, Fritsch D. J Polym Sci Part A Polym Chem 2005;43:6272–81.
[7] Wu S, Hayakawa T, Kikuchi R, Grunzinger SJ, Kakimoto M. Macromolecules 2007;40:5698–705.
[8] Wu S, Hayakawa T, Kakimoto M, Oikawa H. Macromolecules 2008;41:3481–7.
[9] Tao L, Yang H, Liu J, Fan L, Yang S. Polymer 2009;50:6009–18.
[10] Chang CW, Lin CH, Cheng PW, Hwang HJ, Dai SA. J Polym Sci Part A Polym Chem 2009;47:2486–99.
[11] Li FM, Ge JJ, Honigfort PS, Fang S, Chen JC, Harris FW, et al. Polymer 1999;40:4987–5002.
[12] Liaw DJ, Chang FC, Leung MK, Chou MY, Muellen K. Macromolecules 2005;38:4024–9.
[13] Watson KA, Palmieri FL, Connell JW. Macromolecules 2002;35:4968–74.
[14] Kwak SM, Yeon JH, Yoon TH. J Polym Sci Part A Polym Chem 2006;44:2567–78.
[15] Fitch JW, Reddy VS, Youngman PW, Wohlfahrt GA, Cassidy PE. Polymer 2000;41:2301–4.

[16] Jeong KU, Kim JJ, Yoon TH. Polymer 2001;42:6019–30.

[17] Sponto′n M, Ronda JC, Galia` M, Ca′diz V. J Polym Sci Part A Polym Chem 2007;45:2142–51.

[18] Cheng SZ, Chen L, Wang YZ. J Polym Sci Part A Polym Chem 2008;46:5752–5.

[19] Canadell J, Manteco′n A, Ca′diz V. J Polym Sci Part A Polym Chem 2007;45:1980–92.

[20] Canadell J, Manteco′n A, Ca′diz V. J Polym Sci Part A Polym Chem 2007;45:1920–30.

[21] Lin HT, Lin CH, Hu YM, Su WC. Polymer 2009;50:5685–92.

[22] Lin CH, Lin HT, Chang SL, Hwang HJ, Hu YM, Taso YR, et al. Polymer 2009;50:2264–72.

[23] Liou GS, Hsiao SH. J Polym Sci Part A Polym Chem 2001;39:1786–99.

[24] Liu YL. Polymer 2001;42:3445–54.

[25] Lin CH, Lin CH. J Polym Sci Part A Polym Chem 2007;45:2897–912.

[26] Lin CH, Wang CS. Polymer 2001;42:1869–78.

[27] Perez RM, Sandler JKW, Altstädt V, Hoffmann T, Pospiech D, Ciesielski M, et al. Polymer 2007;48:778–90.

[28] Liu YL, Tsai SH. Polymer 2002;43:5757–62.

[29] Kim WG, Hay Allan S. Macromolecules 1993;26:5275–80.

[30] Chung IS, Kim SY. Macromolecules 2000;33:3190–3.

[31] Choi H, Chung IS, Hong K, Park CE, Kim SY. Polymer 2008;49:2644–9.

[32] Hsiao SH, Lin KH. J Polym Sci Part A Polym Chem 2005;43:331–41.

[33] Chern YT, Tsai JY, Wang JJ. J Polym Sci Part A Polym Chem 2009;47:2443–52.

[34] Chern YT, Ju MH. Macromolecules 2009;42:169–79.

[35] Chern YT, Tsai JU. Macromolecules 2008;41:9556–64.

[36] Wang CY, Li G, Jiang JM. Polymer 2009;50:1709–16.

[37] Yi MH, Huang W, Jin MY, Choi KY. Macromolecules 1997;30:5606–11.

[38] Chang YT, Shu CF, Le CM, Wei KH. J Polym Sci Part A Polym Chem 2003;41:3726–35.

[39] Ueda M, Nakayama T. Macromolecules 1996;29:6427–31.

[40] Sinananwanich W, Segawa Y, Higashihara T, Ueda M. Macromolecules 2009. doi:10.1021/ma901708p.

[41] Varma K, Rao BS. J Appl Polym Sci 1983;28:2805–12.

[42] Connell JW, Watson KA. High Perform Polym 2001;13:23.